

The pairing symmetry in quasi-one-dimensional superconductor $\text{Rb}_2\text{Mo}_3\text{As}_3$

Žiga Gosar,^{1,2} Tina Arh,^{1,2} Kevin Jaksetič,¹ Andrej Zorko,^{1,2,*} Wenhao Liu,³
Hanlin Wu,³ Chennan Wang,⁴ Hubertus Luetkens,⁴ Bing Lv,³ and Denis Arčon^{1,2,†}

¹*Institute Jožef Stefan, Jamova 39, SI-1000, Ljubljana, Slovenia*

²*Faculty of mathematics and physics, University of Ljubljana, Jadranska 19, SI-1000, Ljubljana, Slovenia*

³*University of Texas at Dallas, 800 West Campbell Road Richardson, Texas*

⁴*Laboratory for Muon Spin Spectroscopy, Paul Scherrer Institute, CH-5232 Villigen, Switzerland*

(Dated: February 7, 2023)

Quasi-one-dimensional electron systems display intrinsic instability towards long-range ordered phases at sufficiently low temperatures. The superconducting orders are of particular interest as they can possess either singlet or triplet pairing symmetry and frequently compete with magnetism. Here we report on muon spin rotation and relaxation (μSR) study of $\text{Rb}_2\text{Mo}_3\text{As}_3$ characterised by one of the highest critical temperatures $T_c = 10.4$ K among quasi-one-dimensional superconductors. The transverse-field μSR signal shows enhanced damping below T_c due to the formation of vortex lattice. Comparison of vortex lattice broadening against single gap s -, p - and d -wave models shows the best agreement for the s -wave scenario but with the anomalously small superconducting gap, Δ_0 , to T_c ratio of $2\Delta_0/k_B T_c = 2.74(1)$. The alternative nodal p -wave or d -wave scenarios with marginally worse goodness of fit would yield more realistic $2\Delta_0/k_B T_c = 3.50(2)$ and $2\Delta_0/k_B T_c = 4.08(1)$, respectively, and thus they cannot be ruled out when accounting for the superconducting state in $\text{Rb}_2\text{Mo}_3\text{As}_3$.

I. INTRODUCTION

Electron interactions in a one-dimensional (1D) system turn any excitation into a collective one with characteristic power-law dependencies of correlation functions, which is remarkably well described by the Tomonaga-Luttinger liquid (TLL) theory [1–3]. The TLL theory also predicts that electron correlations in 1D trigger fluctuations in the spin-density-wave, charge-density-wave or superconducting order parameters. In realistic quasi-1D systems the weak coupling between chains then stabilizes three-dimensional long-range order at finite temperature. There are only a handful examples of quasi-1D strongly correlated electron systems with competing insulating magnetically ordered and unconventional superconducting states. For example, Bechgaard salts [4, 5] showing strong suppression of superconducting critical temperature, T_c , by disorder [6], the persistence of superconductivity at fields that by far exceed the paramagnetic limit [7] and the absence of characteristic reduction in the NMR Knight shift below T_c [8] have been considered as candidates for the elusive triplet superconductivity.

Recently, $\text{A}_2\text{Cr}_3\text{As}_3$ [9–21] and $\text{A}_2\text{Mo}_3\text{As}_3$ ($\text{A} = \text{K}, \text{Rb}, \text{Cs}$) [22–26] have emerged as new candidates for such quasi-1D superconductors. Their structure comprises assembled Cr_3As_3 or Mo_3As_3 chains separated by alkali metals [9, 22]. First principle calculations emphasise their quasi-1D electronic structure: the Fermi surface consists of two one-dimensional and one three-dimensional components [10, 20, 23, 25]. The presence of 1D features is reflected in their highly anisotropic

transport properties and TLL physics probed for example by nuclear magnetic resonance (NMR) [14, 21, 24]. The emerging superconducting state shows many properties of unconventional superconductors, including the large specific heat jump at T_c and large upper critical fields exceeding the Pauli limit [9, 12], the absence of the Hebel-Slichter coherence peak and the power-law dependence of nuclear spin-lattice relaxation rate $1/T_1$ [14, 15, 24]. Moreover, the transverse field muon spin relaxation (μSR) results on $\text{Cs}_2\text{Cr}_3\text{As}_3$ are more consistent with a nodal gap structure than an isotropic s -wave model for the superconducting gap, while the zero-field μSR relaxation is enhanced below T_c thus hinting to the triplet-type superconductivity [17, 18]. Therefore, the possibility of triplet superconductivity has been discussed in the literature for these two families of materials but the consensus about the pairing symmetry has not been reached yet.

A recent theoretical study suggests that $\text{A}_2\text{Cr}_3\text{As}_3$ with $T_c \sim 6$ K is indeed an unconventional superconductor possibly hosting triplet superconductivity, but the related Mo-analogues $\text{A}_2\text{Mo}_3\text{As}_3$, with higher $T_c \sim 10$ K, should be conventional multigap superconductors [25]. Inelastic neutron scattering seems to corroborate this picture – while antiferromagnetic spin fluctuations are present in both families, they are in the superconducting state of $\text{K}_2\text{Cr}_3\text{As}_3$ gapless, but gapped in $\text{K}_2\text{Mo}_3\text{As}_3$ [26]. In the latter case the gap opens below ~ 6 K for energies below ~ 5 meV. Although the data does not allow to unambiguously discriminate between nodal or nodeless gap functions, it has been argued that $\text{K}_2\text{Mo}_3\text{As}_3$ may belong to conventional superconductors as theoretically suggested. That would imply the leading role of a three-dimensional Fermi surface for the occurrence of superconductivity. On the other hand, power-law dependence of ^{87}Rb $1/T_1$ in $\text{Rb}_2\text{Mo}_3\text{As}_3$ underlines the impor-

* andrej.zorko@ijs.si

† denis.arcon@ijs.si

tance of 1D Fermi surface components carrying TLL as a parent state for the low-temperature unconventional superconductivity [24].

To throw some additional light on apparently contradicting experiments and theory we here report a μ SR study of $\text{Rb}_2\text{Mo}_3\text{As}_3$. We estimate the Ginzburg–Landau parameter $\kappa \approx 200$ that classifies $\text{Rb}_2\text{Mo}_3\text{As}_3$ as a strong type-II superconductor in the clean limit. More importantly, transverse field (TF) μ SR allows us to determine the temperature dependence of the magnetic penetration depth. The superconducting contribution to the TF μ SR relaxation does not show any signs of saturation down to $T/T_c \sim 0.14$, which is generally incompatible with a single-gap s -wave model. Furthermore, forcing this model of conventional superconductivity yields an anomalously small superconducting gap, Δ_0 , to T_c ratio $2\Delta_0/k_B T_c = 2.74(1)$. On the other hand, almost equally good fits are obtained for the nodal p -wave or d -wave scenarios with much more realistic $2\Delta_0/k_B T_c = 3.50(2)$ and $2\Delta_0/k_B T_c = 4.08(1)$, respectively. Present results do not definitely rule out the conventional s -wave scenario, but also keep the door wide open for the unconventional nodal-type superconductivity in $\text{Rb}_2\text{Mo}_3\text{As}_3$.

II. EXPERIMENTAL METHODS

Preparation of polycrystalline $\text{Rb}_2\text{Mo}_3\text{As}_3$ followed the same steps as reported previously [24]. Laboratory powder X-ray diffraction suggested a phase pure sample with a hexagonal crystal lattice and space group $P\bar{6}m2$. High sample quality was further confirmed by dc magnetic susceptibility measurements in the zero-field cooling protocol at $\mu_0 H = 1$ mT, which showed bulk superconductivity below $T_c = 10.4$ K with a diamagnetic shielding fraction of almost 100%. To avoid any possible sample degradation we strictly avoided the exposure of samples to air at all stages - sample handling and packing was done in Ar-filled glove box with a control atmosphere where O_2 and H_2O contents were below 0.1 ppm and sample was transported between experimental sites in a glass tube sealed under high vacuum.

All μ SR measurements were conducted on the GPS instrument at the Paul Scherrer Institut (PSI), Switzerland [27]. Polycrystalline sample in the form of a pellet with dimensions 5 mm in diameter and 4 mm thick was sealed between two layers of kapton tape in a glovebox and then glued to a fork sample holder made of copper. μ SR measurements were done in veto mode, thus minimizing the background signal to below $\sim 5\}$. Measurements of μ SR signal were performed in the zero-field (ZF), longitudinal field (LF) and TF geometries [28]. Stray fields from the Earth or from the neighbouring instruments were cancelled in ZF measurements with adaptive compensation coils. The majority of the TF μ SR experiments were undertaken in a magnetic field of 100 mT, which is above H_{c1} and well below H_{c2} . In our measurements we thermalised the sample at each temperature prior the start

of the measurement and used high statistics with about 20 million events for each dataset. Raw μ SR data were analysed using `musrfit` software [29].

III. RESULTS

To determine the temperature dependence of the superfluid density, we first measured TF μ SR above and below T_c using the standard field cooling (FC) thermal protocol. Characteristic TF μ SR asymmetries taken at $T = 11$ K (just above T_c) and at $T = 1.5$ K (well below T_c) are compared in Fig. 1. The relaxation of TF μ SR signal above T_c is very weak and mainly originates from the dipolar coupling to small static nuclear moments. Below T_c , the relaxation of TF μ SR signal is significantly enhanced. This is a signature of the vortex lattice formation leading to inhomogeneous field distribution at the implanted muon sites.

Fourier transform of the TF μ SR data yields spectra with a sharp line at the applied field and a broader component shifted to lower fields (not shown). The former, much less intense signal is likely due to muons stopping either in a parasitic non-superconducting phase or in the sample holder, while the broader component shifted to lower fields originates from the sample in the superconducting state. Both components can be well described by a Gaussian lineshape. The expected asymmetric lineshape broadening of the superconducting component [30] was also tested by assuming skewed Gaussian lineshape [29] but the resulting asymmetry in the widths was very small. We thus analyze the TF μ SR data at all tempera-

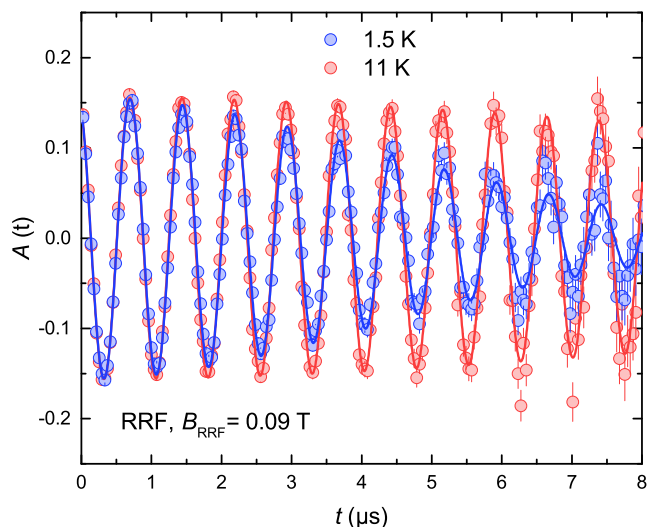


FIG. 1. Transverse field (TF) μ SR measurements of $\text{Rb}_2\text{Mo}_3\text{As}_3$ in a field of 100 mT at temperatures $T = 11$ K (red), i.e., above $T_c = 10.4$ K and $T = 1.5$ K (blue). Solid red and blue lines are fits to Eq. 1. The plot is shown in rotating reference frame (RRF) with the frequency that corresponds to 90 mT.

tures with two components, both experiencing Gaussian relaxation,

$$A(t) = A[(1 - f) \exp \left[-\frac{1}{2}(\sigma t)^2 \right] \cos(2\pi\nu t + \varphi) + F \exp \left[-\frac{1}{2}(\sigma_b t)^2 \right] \cos(2\pi\nu_b t + \varphi)]. \quad (1)$$

Here σ and σ_b are the Gaussian relaxation rates for the sample and background components, respectively, ν and ν_b are the respective muon precession frequencies, φ is the phase given by the detector geometries and $F = 0.148$ is the fraction of the background signal. The latter was determined for the data collected at $T = 1.5$ K and then kept constant for all other temperatures. The relaxation rate of the background component $\sigma_b = 0.158 \mu\text{s}^{-1}$ and its resonance field $2\pi\nu_b/\gamma_\mu = 99.887$ mT were also fixed.

These assumptions allowed us to determine the temperature dependencies of the experimental frequency shift, $K = (\nu - \nu_b)/\nu_b$, measured against ν_b and the corresponding relaxation rate, σ , of the $\text{Rb}_2\text{Mo}_3\text{As}_3$ sample in the FC experiment (Fig. 2). The μSR spectrum of the superconducting component starts to diamagnetically shift at $T_c = 10.4$ K (Fig. 2a). The muon relaxation rate gets enhanced just below T_c and $\sigma(T)$ monotonically increases with lowering temperature (Fig. 2b), but does never really saturate even at $T/T_c \approx 0.14$.

The relaxation rate σ of muons implanted in sample has two contributions: the temperature-dependent contribution from the vortex lattice, which is dominant in the superconducting phase, σ_{sc} , and the smaller temperature-independent contribution from the nuclear dipole moments, σ_n . The total Gaussian relaxation rate is then given by $\sigma = \sqrt{\sigma_{sc}^2 + \sigma_n^2}$ [17, 18, 31–33]. Above T_c , $\sigma_{sc} = 0$, which allows us to determine $\sigma_n = 0.064 \mu\text{s}^{-1}$.

As the applied TF field of 100 mT is much smaller than the upper critical field $\mu_0 H_{c2} \approx 28$ T, we can use the calculated value of $\sigma_{sc} = 0.24 \mu\text{s}^{-1}$ at $T = 1.5$ K to estimate the effective penetration depth, $\lambda = \sqrt{0.0609\gamma_\mu\Phi_0/\sigma_{sc}} = 669$ nm [34]. Here Φ_0 is the magnetic flux quantum and γ_μ is the muon gyromagnetic ratio. Taking into consideration also the coherence length $\zeta = 3.4$ nm, estimated from H_{c2} , this yields the Ginzburg–Landau parameter $\kappa = \lambda/\zeta \approx 200$ and classifies $\text{Rb}_2\text{Mo}_3\text{As}_3$ as a strong type-II superconductor. We note that the above expression for the effective penetration depth holds for $0.13/\kappa^2 \ll (H/H_{c2}) \ll 1$ and $\kappa \gg 70$ [34], which is well justified in our TF experiments. Finally, the carrier mean free path calculated based on resistivity data [24] is $l_{\text{eff}} \approx 20$ nm, thus the studied compound seems to be in the clean limit.

$\text{Rb}_2\text{Mo}_3\text{As}_3$ is a quasi-1D superconductor and thus the anisotropy of the penetration depths $\gamma_\lambda = \lambda_c/\lambda_{ab}$ could be present. Here λ_c and λ_{ab} are the penetration depths along the chain and in the plane perpendicular to the chains, respectively. In such cases, the effective penetration depth may differ from λ_{ab} and λ_c by a factor close to 1 [31], but this should not affect the overall temperature dependence of σ_{sc} . In any case, the anisotropy of

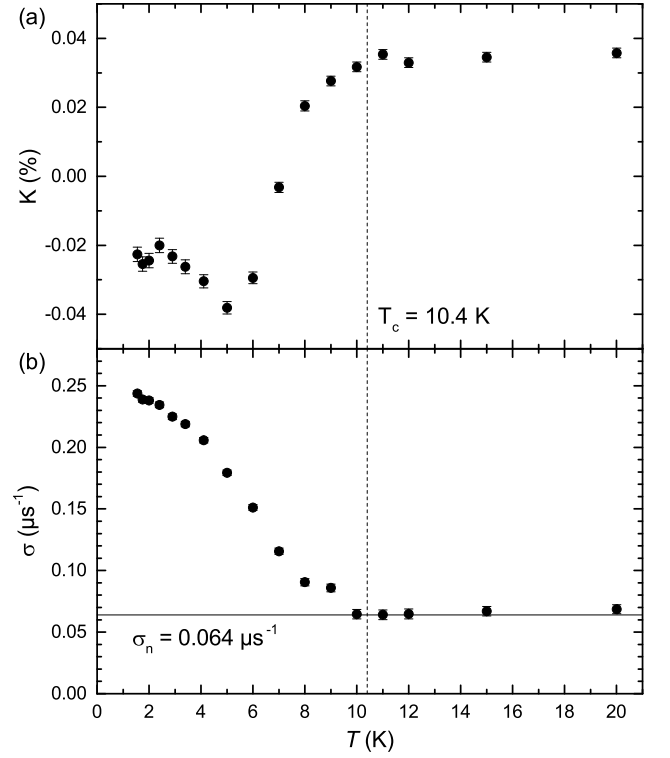


FIG. 2. (a) The temperature dependence of the experimental frequency shift, K , in the quasi-one-dimensional $\text{Rb}_2\text{Mo}_3\text{As}_3$ superconductor obtained from the fits of TF μSR data with Eq. 1. (b) The temperature dependence of TF μSR Gaussian relaxation rates, σ . The magnetic field was set to 100 mT and the data corresponds to the measurements collected after the field-cooled protocol. The vertical dashed line marks $T_c = 10.4$ K, while the solid horizontal line in (b) indicates the nuclear contribution to the TF μSR relaxation, $\sigma_n = 0.064 \mu\text{s}^{-1}$.

the iron-pnictide superconductors is usually found to be small [35] and thus we speculate that the effective λ is not much different from λ_c and λ_{ab} . Therefore, we proceed with our analysis using the effective $\lambda(T)$ which is inversely proportional to the square root of σ_{sc} and relate it to the superfluid density and its temperature dependence [33],

$$\frac{\sigma_{sc}(T)}{\sigma_{sc}(0)} = 1 + \frac{1}{\pi} \int_0^{2\pi} \int_{\Delta(T,\phi)}^{\infty} \frac{\partial f}{\partial E} \frac{EdEd\phi}{\sqrt{E^2 - \Delta^2(T,\phi)}}. \quad (2)$$

Here $f = [1 + \exp(-E/k_B T)]^{-1}$ is the Fermi function. The superconducting gap is temperature and angular dependent through $\Delta(T, \phi) = \Delta_0 \delta(T/T_c) g(\phi)$ [11]. Δ_0 is the maximum gap value at $T = 0$. Following the literature, we use the BCS expression for the temperature dependence of the superconducting gap $\delta(T/T_c) = \tanh[1.82 \cdot (1.018(T_c/T - 1))^{0.51}]$ [36]. With ϕ as an azimuthal angle along the Fermi surface, $g(\phi)$ takes into account the angular dependence of the superconducting gap. In our modeling we assumed isotropic (s -wave) $g(\phi) = 1$, $g(\phi) = |\cos(\phi)|$ for the p -wave, and $g(\phi) =$

$|\cos(2\phi)|$ for the d -wave nodal gaps.

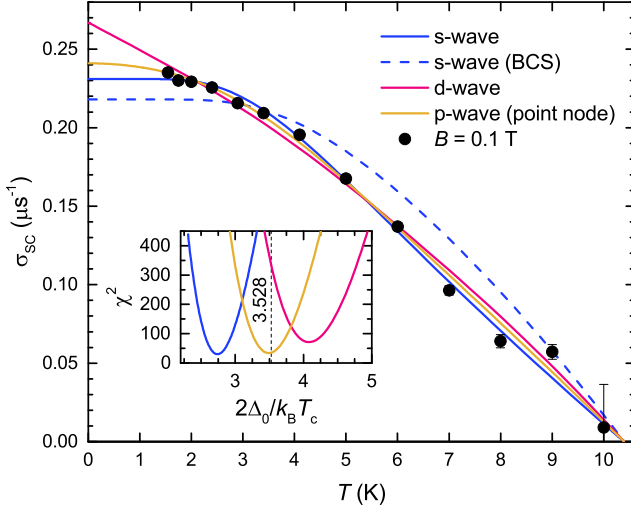


FIG. 3. The temperature dependence of the TF μ SR superconducting relaxation rate, σ_{sc} (black circles). Dashed blue line is the calculated $\sigma_{sc}(T)$ for the s -wave scenario with the BCS value of the superconducting gap, Δ_0 , to T_c ratio $2\Delta_0/k_B T_c = 3.528$. Solid blue, orange and pink lines correspond to s -, and nodal p - and d -waves with the optimized $2\Delta_0/k_B T_c$ values, respectively. Inset: Variation of the goodness of fit χ^2 against $2\Delta_0/k_B T_c$ values for all three single-gap models.

The temperature dependence of $\sigma_{sc}(T)$ is in Fig. 3 compared against different single-gap models computed from Eq. 2. It is immediately evident that the conventional single-gap s -wave model with the weak-coupling BCS value of the superconducting gap to T_c ratio $2\Delta_0/k_B T_c = 3.528$ completely fails in describing the data. The goodness of fit, χ^2 , is significantly improved (from previous $\chi^2 > 400$ to $\chi^2 = 30.2$) if the superconducting gap is reduced to $\Delta_0/k_B = 14.2(1)$ K so that $2\Delta_0/k_B T_c = 2.74(1)$ (inset to Fig. 3). We stress that this gap value is significantly smaller than it is predicted by the conventional BCS value. We also tested anisotropic s -wave (but nodeless) model, but this model also converges to values of $2\Delta_0/k_B T_c$ much smaller than the BCS value. Remarkably, the point nodal p -wave model gives only marginally worse $\chi^2 = 33.8$, but for $\Delta_0/k_B = 18.2(1)$ K and thus more reasonable $2\Delta_0/k_B T_c = 3.50(2)$. This model also agrees better with the observation that $\sigma_{sc}(T)$ does not show any signs of saturation down to $T/T_c \approx 0.14$. Finally, we tested also the line nodal d -wave model that shows somewhat worse $\chi^2 = 71.1$ for the optimised $2\Delta_0/k_B T_c = 4.08(1)$.

As the Fermi surface of $\text{Rb}_2\text{Mo}_3\text{As}_3$ comprises two quasi-1D and one three-dimensional components, we tried also the two-gap $s + s$ -wave model. We assumed a weighted sum of two normalised superfluid densities calculated from Eq. 2 to obtain

$$\sigma_{sc}(T) = w\sigma_{sc}(\Delta_1, T) + (1 - w)\sigma_{sc}(\Delta_2, T). \quad (3)$$

To minimise the number of free parameters, the first component with the BCS superconducting gap $2\Delta_1/T_c = 3.528$ was fixed. Its weight, w , and the value of $2\Delta_2/T_c$ for the second component with a smaller superconducting gap Δ_2 was used to minimise χ^2 . The parameter optimisation spontaneously converged to a very small weight of the BCS-component, i.e., to $w = 0.1$ and $2\Delta_2/k_B T_c = 2.67$ ($\chi^2 = 29.6$). The marginal weight for the component with the larger Δ_1 shows that the two-gap model is essentially very similar to the solution with a single anomalously small s -wave gap as discussed above.

Since the p -wave single gap model appears as a strong candidate to fit TF μ SR data, we next focus on ZF μ SR measurements to test possible time-reversal symmetry-breaking superconducting state. In Fig. 4 we compare ZF- μ SR data collected above T_c at $T = 15$ K to data accumulated well below T_c at $T = 1.5$ K. For both temperatures the data can be reasonably fit to a simple exponential decay function

$$A(t) = A_0 \exp(-\lambda_{ZF} t). \quad (4)$$

Here A_0 is the initial asymmetry, while λ_{ZF} is the muon spin relaxation rate due to local magnetic fields. Fitting ZF μ SR data to the expression Eq. 4 shows that λ_{ZF} is slightly enhanced in the superconducting state: $\lambda_{ZF} = 0.047(1) \mu\text{s}^{-1}$ at 15 K increases to $\lambda_{ZF} = 0.052(1) \mu\text{s}^{-1}$ at 1.5 K. The muon spin relaxation is quickly suppressed already in small longitudinal fields of 10 mT (Fig. 4) implying slow local field fluctuations or even quasi-static local fields, as usually originating from nuclei. Even if the unknown background contribution is added to Eq. 4, the extracted value of λ_{ZF} for $T = 1.5$ K would still be larger compared to that for the $T = 15$ K dataset. For example, with 5% of background included, as it might be expected for our experimental setup, λ_{ZF} changes to $0.050(2) \mu\text{s}^{-1}$ and $0.055(2) \mu\text{s}^{-1}$ for $T = 1.5$ K and $T = 15$ K, respectively. The minute enhancement in λ_{ZF} in the superconducting state seems to be within the uncertainty of current experiments and does not allow to unambiguously confirm the conjecture of time reversal symmetry-breaking superconducting state.

IV. DISCUSSION AND CONCLUSIONS

The main experimental findings of the present μ SR study of the quasi-1D superconductor $\text{Rb}_2\text{Mo}_3\text{As}_3$ may be summarised as follows: (i) the vortex-lattice contribution to the Gaussian relaxation rate does not show any saturation even for $T/T_c \approx 0.14$, (ii) the TF μ SR frequency shift shows the diamagnetic shift below T/T_c , but also an anomaly at ~ 6 K, (iii) the ZF relaxation seems to be marginally enhanced at $T = 1.5$ K compared to that measured above T_c at $T = 15$ K. Should the conventional superconductivity scenario apply to $\text{Rb}_2\text{Mo}_3\text{As}_3$, then the small relative gap value, $2\Delta_0/k_B T_c = 2.74(1)$, needs to be explained. It also appears that the modeling of TF

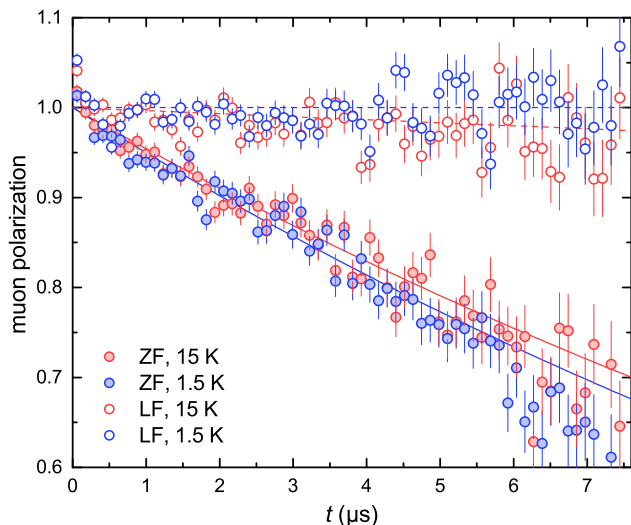


FIG. 4. The time dependence of the zero-field (ZF) μ SR (solid circles) and weak 10 mT longitudinal-field (LF) (open circles) muon polarization collected above T_c at $T = 15$ K (red symbols) and well below T_c at $T = 1.5$ K (blue symbols). Solid lines are fits of the ZF and dashed lines of the LF μ SR data to a simple exponential decay function (Eq. 4).

μ SR relaxation rate using nodeless anisotropic s -wave or two-gap $s + s$ -wave models does not resolve the issue of anomalously small Δ_0 . We note that the similarly small ratio $2\Delta_0/k_B T_c$ as found by μ SR has been previously deduced also from our ^{87}Rb NMR data [24]. As possible explanation for the anomalous $2\Delta_0/k_B T_c < 3.528$ extracted from NMR data, we previously considered the gap averaging due to impurity scattering and a weighted average of the relaxation in the vortex core and in the inter-vortex region.

However, the present μ SR analysis shows that the nodal-superconductivity scenario is also possible for $\text{Rb}_2\text{Mo}_3\text{As}_3$. The temperature dependence of σ_{sc} and the minute enhancement of λ_{ZF} in the superconducting state are both compliant with the p -wave superconductivity. The enhancement in λ_{ZF} below T_c by $5 \cdot 10^{-3} \mu\text{s}^{-1}$ is sim-

ilar to that observed in the sister compound $\text{Cs}_2\text{Cr}_3\text{As}_3$ and 20 times larger than in $\text{K}_2\text{Cr}_3\text{As}_3$ [18]. Despite the similarity in the ZF μ SR data between the Mo- and Cr-based families, it has to be stressed though that more detailed measurements are needed to unambiguously confirm enhancement in λ_{ZF} in the case of $\text{Rb}_2\text{Mo}_3\text{As}_3$. If the nodal-superconductivity scenario for $\text{Rb}_2\text{Mo}_3\text{As}_3$ is correct, then the anomaly in the TF μ SR frequency shift below ~ 6 K may indicate a weak internal field due to the presence of the triplet superconducting component. Interestingly, we note that inelastic neutron scattering data indicate the opening of the superconducting gap below ~ 6 K in $\text{K}_2\text{Mo}_3\text{As}_3$, although it has a similar $T_c \approx 10$ K [26] as $\text{Rb}_2\text{Mo}_3\text{As}_3$ studied here.

While NMR, NQR and now also μ SR techniques seem to be consistent when probing the superconducting state of $\text{Rb}_2\text{Mo}_3\text{As}_3$, one cannot overlook the apparent inconsistencies with the inelastic neutron scattering [26] or with first principle calculations [25]. For example, the superconducting gap deduced from all three local-probe methods is around $\Delta_0 \approx 1.2$ meV, which is much less than 3.1 meV extracted from the neutron scattering. As magnetic resonance methods are very sensitive to low-energy excitations, they offer *a priori* better energy resolution in this energy range. More precise μ SR experiments extended to $T/T_c \ll 0.1$ are therefore desired to ultimately address the symmetry of the superconducting order parameter in the $\text{Rb}_2\text{Mo}_3\text{As}_3$ quasi-1D superconductor.

ACKNOWLEDGMENTS

DA wishes to acknowledge the support of the Slovenian research agency through research program No. P1-0125 and research projects N1-0220 and J1-3007. AZ acknowledges the support of the Slovenian research agency through the research project N1-0148. This work at University of Texas at Dallas is supported by US Air Force Office of Scientific Research Grant No. FA9550-19-1-0037 and National Science Foundation (NSF)-DMREF-1921581.

[1] T. Giamarchi and H. J. Schulz, Anderson localization and interactions in one-dimensional metals, *Phys. Rev. B* **37**, 325 (1988).
[2] T. Giamarchi, *Quantum Physics in One Dimension*, International Series of Monographs on Physics (Clarendon Press, 2003).
[3] H. J. Schulz, G. Cuniberti, and P. Pieri, Fermi liquids and Luttinger liquids, in *Field theories for low-dimensional condensed matter systems* (Springer, 2000) pp. 9–81.
[4] D. Jérôme and H. J. Schulz, Organic conductors and superconductors, *Advances in Physics* **51**, 293 (2002).
[5] S. Brown, Organic superconductors: The Bechgaard salts and relatives,

Physica C: Superconductivity and its Applications **514**, 279 (2015).
[6] M. Y. Choi, P. M. Chaikin, S. Z. Huang, P. Haen, E. M. Engler, and R. L. Greene, Effect of radiation damage on the metal-insulator transition and low-temperature transport in the tetramethyltetraselenofulvalinium PF_6 salt $[(\text{TMTSF})_2\text{PF}_6]$, *Phys. Rev. B* **25**, 6208 (1982).
[7] I. J. Lee, M. J. Naughton, G. M. Danner, and P. M. Chaikin, Anisotropy of the Upper Critical Field in $(\text{TMTSF})_2\text{PF}_6$, *Phys. Rev. Lett.* **78**, 3555 (1997).
[8] I. J. Lee, S. E. Brown, W. G. Clark, M. J. Strouse, M. J. Naughton, W. Kang, and P. M. Chaikin, Triplet Superconductivity in an Organic Superconductor Probed by NMR Knight Shift, *Phys. Rev. Lett.* **88**, 017004 (2001).

- [9] J.-K. Bao, J.-Y. Liu, C.-W. Ma, Z.-H. Meng, Z.-T. Tang, Y.-L. Sun, H.-F. Zhai, H. Jiang, H. Bai, C.-M. Feng, Z.-A. Xu, and G.-H. Cao, Superconductivity in Quasi-One-Dimensional $\text{K}_2\text{Cr}_3\text{As}_3$ with Significant Electron Correlations, *Phys. Rev. X* **5**, 011013 (2015).
- [10] X. Wu, F. Yang, C. Le, H. Fan, and J. Hu, Triplet p_z -wave pairing in quasi-one-dimensional $\text{A}_2\text{Cr}_3\text{As}_3$ superconductors ($\text{A} = \text{K}, \text{Rb}, \text{Cs}$), *Phys. Rev. B* **92**, 104511 (2015).
- [11] G. M. Pang, M. Smidman, W. B. Jiang, J. K. Bao, Z. F. Weng, Y. F. Wang, L. Jiao, J. L. Zhang, G. H. Cao, and H. Q. Yuan, Evidence for nodal superconductivity in quasi-one-dimensional $\text{K}_2\text{Cr}_3\text{As}_3$, *Phys. Rev. B* **91**, 220502 (2015).
- [12] Z.-T. Tang, J.-K. Bao, Y. Liu, Y.-L. Sun, A. Ablimit, H.-F. Zhai, H. Jiang, C.-M. Feng, Z.-A. Xu, and G.-H. Cao, Unconventional superconductivity in quasi-one-dimensional $\text{Rb}_2\text{Cr}_3\text{As}_3$, *Phys. Rev. B* **91**, 020506 (2015).
- [13] M. D. Watson, Y. Feng, C. W. Nicholson, C. Monney, J. M. Riley, H. Iwasawa, K. Refson, V. Sacksteder, D. T. Adroja, J. Zhao, and M. Hoesch, Multiband One-Dimensional Electronic Structure and Spectroscopic Signature of Tomonaga-Luttinger Liquid Behavior in $\text{K}_2\text{Cr}_3\text{As}_3$, *Phys. Rev. Lett.* **118**, 097002 (2017).
- [14] H. Zhi, D. Lee, T. Imai, Z. Tang, Y. Liu, and G. Cao, ^{133}Cs and ^{75}As NMR investigation of the normal metallic state of quasi-one-dimensional $\text{Cs}_2\text{Cr}_3\text{As}_3$, *Phys. Rev. B* **93**, 174508 (2016).
- [15] H. Z. Zhi, T. Imai, F. L. Ning, J.-K. Bao, and G.-H. Cao, NMR Investigation of the Quasi-One-Dimensional Superconductor $\text{K}_2\text{Cr}_3\text{As}_3$, *Phys. Rev. Lett.* **114**, 147004 (2015).
- [16] G. M. Pang, M. Smidman, W. B. Jiang, J. K. Bao, Z. F. Weng, Y. F. Wang, L. Jiao, J. L. Zhang, G. H. Cao, and H. Q. Yuan, Evidence for nodal superconductivity in quasi-one-dimensional $\text{K}_2\text{Cr}_3\text{As}_3$, *Phys. Rev. B* **91**, 220502 (2015).
- [17] D. T. Adroja, A. Bhattacharyya, M. Telling, Y. Feng, M. Smidman, B. Pan, J. Zhao, A. D. Hillier, F. L. Pratt, and A. M. Strydom, Superconducting ground state of quasi-one-dimensional $\text{K}_2\text{Cr}_3\text{As}_3$ investigated using μSR measurements, *Phys. Rev. B* **92**, 134505 (2015).
- [18] D. Adroja, A. Bhattacharyya, M. Smidman, A. Hillier, Y. Feng, B. Pan, J. Zhao, M. R. Lees, A. Strydom, and P. K. Biswas, Nodal Superconducting Gap Structure in the Quasi-One-Dimensional $\text{Cs}_2\text{Cr}_3\text{As}_3$ Investigated Using μSR Measurements, *Journal of the Physical Society of Japan* **86**, 044710 (2017).
- [19] K. M. Taddei, Q. Zheng, A. S. Sefat, and C. de la Cruz, Coupling of structure to magnetic and superconducting orders in quasi-one-dimensional $\text{K}_2\text{Cr}_3\text{As}_3$, *Phys. Rev. B* **96**, 180506 (2017).
- [20] C. Xu, N. Wu, G.-X. Zhi, B.-H. Lei, X. Duan, F. Ning, C. Cao, and Q. Chen, Coexistence of non-trivial topological properties and strong ferromagnetic fluctuations in quasi-one-dimensional $\text{A}_2\text{Cr}_3\text{As}_3$, *npj Computational Materials* **6**, 1 (2020).
- [21] J. Yang, J. Luo, C. Yi, Y. Shi, Y. Zhou, and G. qing Zheng, Spin-triplet superconductivity in $\text{K}_2\text{Cr}_3\text{As}_3$, *Science Advances* **7**, eabl4432 (2021).
- [22] Q.-G. Mu, B.-B. Ruan, K. Zhao, B.-J. Pan, T. Liu, L. Shan, G.-F. Chen, and Z.-A. Ren, Superconductivity at 10.4 K in a novel quasi-one-dimensional ternary molybdenum pnictide $\text{K}_2\text{Mo}_3\text{As}_3$, *Science Bulletin* **63**, 952 (2018).
- [23] Y. Yang, S.-Q. Feng, H.-Y. Lu, W.-S. Wang, and Z.-P. Chen, Electronic Structures of Newly Discovered Quasi-One-Dimensional Superconductors $\text{A}_2\text{Mo}_3\text{As}_3$ ($\text{A}=\text{K}, \text{Rb}, \text{Cs}$), *J. Supercond. Nov. Magn.* **32**, 2421 (2019).
- [24] Z. Gosar, N. Janša, T. Arh, P. Jeglič, M. Klanjšek, H. F. Zhai, B. Lv, and D. Arčon, Superconductivity in the regime of attractive interactions in the Tomonaga-Luttinger liquid, *Phys. Rev. B* **101**, 220508 (2020).
- [25] B.-H. Lei and D. J. Singh, Multigap electron-phonon superconductivity in the quasi-one-dimensional pnictide $\text{K}_2\text{Mo}_3\text{As}_3$, *Phys. Rev. B* **103**, 094512 (2021).
- [26] K. M. Taddei, B.-H. Lei, M. A. Susner, H.-F. Zhai, T. J. Bullard, L. D. Sanjeewa, Q. Zheng, A. S. Sefat, S. Chi, C. d. Cruz, D. J. Singh, and B. Lv, Gapless spin-excitations in the superconducting state of a quasi-one- (2022).
- [27] A. Amato, H. Luetkens, K. Sedlak, A. Stoykov, R. Scheuermann, M. Elender, A. Raselli, and D. Graf, The new versatile general purpose surface-muon instrument (GPS) based on silicon photomultipliers for μSR measurements on a continuous-wave beam, *Review of Scientific Instruments* **88**, 093301 (2017).
- [28] A. Yaouanc and P. D. De Reotier, *Muon spin rotation, relaxation, and resonance: applications to condensed matter* (Oxford University Press, Oxford, 2011).
- [29] A. Suter and B. Wojek, Musrfit: A Free Platform-Independent Framework for μSR Data Analysis, *Physics Procedia* **30**, 69 (2012).
- [30] A. Maisuradze, R. Khasanov, A. Shengelaya, and H. Keller, Comparison of different methods for analyzing μSR line shapes in the vortex state of type-II superconductors, *Journal of Physics: Condensed Matter* **21**, 075701 (2009).
- [31] D. T. Adroja, F. K. Kirschner, F. Lang, M. Smidman, A. D. Hillier, Z.-C. Wang, G.-H. Cao, G. B. Stenning, and S. J. Blundell, Multigap superconductivity in $\text{RbCa}_2\text{Fe}_4\text{As}_4\text{F}_2$ investigated using μSR measurements, *Journal of the Physical Society of Japan* **87**, 124705 (2018).
- [32] P. K. Biswas, A. Kreisel, Q. Wang, D. T. Adroja, A. D. Hillier, J. Zhao, R. Khasanov, J.-C. Orain, A. Amato, and E. Morenzoni, Evidence of nodal gap structure in the basal plane of the FeSe superconductor, *Phys. Rev. B* **98**, 180501 (2018).
- [33] R. Prozorov and R. W. Giannetta, Magnetic penetration depth in unconventional superconductors, *Superconductor Science and Technology* **19**, R41 (2006).
- [34] E. H. Brandt, Properties of the ideal Ginzburg-Landau vortex lattice, *Phys. Rev. B* **68**, 054506 (2003).
- [35] H. Q. Yuan, J. Singleton, F. F. Balakirev, S. A. Baily, G. F. Chen, J. L. Luo, and N. L. Wang, Nearly isotropic superconductivity in $(\text{Ba}, \text{K})\text{Fe}_2\text{As}_2$, *Nature* **457**, 565 (2009).
- [36] A. Carrington and F. Manzano, Magnetic penetration depth of MgB_2 , *Physica C: Superconductivity* **385**, 205 (2003).